Effect of voids on the bending response of buried flexible utility pipes

Heather Sales
Cementation Skanska, Doncaster, United Kingdom

Jonathan A. Black & Richard P. Collins
Dept. of Civil & Structural Engineering, University of Sheffield, Sheffield, United Kingdom

GEOQuébec 2015
Challenges from North to South
Des défis du Nord au Sud

ABSTRACT
Buried pipe infrastructure is of critical importance for the provision of fresh water supply and disposal of waste water. Pipe performance is sensitive to initial ground burial conditions and subsequent changes during serviceable life. Voids are frequently reported as a possible factor that accelerates deterioration of the pipe condition leading to ultimate premature failure in flexure or cracking. This study considers the effect of voids on a 0.3 m prototype flexible pipe for fully supported and unsupported conditions buried in sand using centrifuge model tests. Pipe stiffness and bending response for spherical void geometries 2 to 5 times that of the pipe diameter are evaluated when subjected to vertical surface loading. Digital image correlation is used to capture soil-pipe interaction mechanics. Increased pipe deformation and bending moment were observed with increased void size confirming that void formation may contribute in the overall failure of pipe infrastructure.

RÉSUMÉ
Infrastructure de canalisation enterrée est d'une importance critique pour la fourniture de l'approvisionnement en eau douce et l'élimination des eaux usées. Performances Pipe est sensible aux conditions initiales du rez-de sépulture et les changements ultérieurs pendant la vie utile. Les vides sont fréquemment signalés comme un facteur possible qui accélère la détérioration de l'état du tuyau conduisant à une défaillance prématurée ultime en flexion ou de fissuration. Cette étude considère l'effet de vides sur une conduite flexible de 0.3 m prototype utilisant des tests de modèles de centrifugeuses pour conditions entièrement pris en charge et non pris en charge enfouis dans le sable. Rigidité du tuyau et de la réponse de flexion pour des géométries vides sphériques de 2 à 5 du diamètre du tuyau sont évalués lorsqu'ils sont soumis à la verticale de chargement de surface. Corrélation d'image numérique a été utilisé pour capturer sol-tuyaux mécanique d'interaction. La déformation de la conduite accrue et moment de flexion où observée avec augmentation de la taille nulle confirmant que la formation de vides peut contribuer à l'échec global de l'infrastructure de la conduite.

1 INTRODUCTION

Buried pipes form a critical part of civil engineering infrastructure and their number, complexity and density will only increase with continued urbanisation and development (Kellogg, 1993). Buried flexible pipes have applications in utility services such as water supply, sewerage, oil and natural gas distribution. In addition to maintaining and preserving existing assets, new networks are constantly being deployed to meet growing population needs and end user demand.

It is not uncommon that many water distribution systems currently in service contain pipes in excess of 100 years old which presents increased risk of failure (Ratnayaka, 2009). Leakage from fresh water systems is a major concern across the developed world as up to 30% of clean potable water can be lost (Ratnayaka, 2009). Furthermore, failure of fresh and waste water systems presents additional risk of cross-contamination of potable and natural ground water aquifers. The provision and security of water supply is a significant issue for many nations and action is needed to better understand factors that lead to pipe failure in order to effectively manage water distribution and recovery systems responsibly and to boost their future resilience.

Water pipes are typically installed in trenches of compacted backfill which offer confinement and structural support to the pipe. Unlike rigid pipes, flexible pipes can easily deform if unsupported and therefore they rely on the surrounding backfill to develop bending resistance. The design of flexible pipes is typically based on deflection and buckling capacities (i.e. AWWA 1998); whereby both the soil and pipe stiffness are critical in providing structural integrity and preventing failure. Consequently, pipes are highly sensitive to ground movements and temporal changes in soil conditions, both of which are commonly associated with leakage (Tan and Moore, 2007). While standards such as ASTM C443 2005) and BSI (1998) have focused on improving aspects of pipe design such as joint integrity and gasket design, there is still considerable uncertainty about the influence of external factors and their impact on pipe behaviour and failure (Figure 1). A number of common uncertainties include:

(i) the effect of increased stresses on pipes through the transmission of surface loads.
(ii) the role of void formation and subsequent loss of support locally around the pipe perimeter.
(iii) variation in soil conditions in the near surface reactive zone arising from moisture content or temperature changes.

(iv) deterioration of pipe structure from interaction with new infrastructure construction

There are few studies into the effect that the presence of a void has on buried pipes, and fewer still that employ physical modelling techniques. Several numerical investigations into related matters have been carried out by Rajani and Tesfamariam (2004), Zhang et al., (2012) and Tan and Moore (2007). The latter work investigated the effect of backfill erosion on moments in buried rigid pipes using elastic and elastic-plastic finite element analyses. Parametric investigations included the effect of void size, location and shape, which determined that increasing void size increased bending moments in the pipe. Tan and Moore (2007) also stipulated that the rate of bending moment increase amplified rapidly once the void reached a critical size related to the pipe diameter. Additional studies on soil spatial variability are reported by Klar et al. (2005).

Experimental studies by Marshall, (2009) evaluated the effect of tunnelling on buried pipes which compared well with theoretical models. In this work rigid, intermediate and flexible pipes were considered. Other works into pipe-soil interaction for pipe bursting behaviour are reported by Brachman et al. (2010), while more recently Rakitin and Xu (2014) present centrifuge model tests to evaluate the impact of surface traffic loading on large-diameter pipes. Also, Becerril and Moore (2015) performed laboratory tests on a jointed pipeline subjecting it to surface live loads. They concluded that depending on the magnitude and the location of the surface live load relative to the joint, the joint would exhibit rotation or shear displacement between the connected pipe sections.

This study considers the bending behaviour of a flexible supported and unsupported pipe (i.e. void) in sand using centrifuge model testing. Bending response is evaluated for a spherical void of increasing volume located beneath the pipe, subjected to vertical surface load designed to simulate a single truck/lorry axle loading.

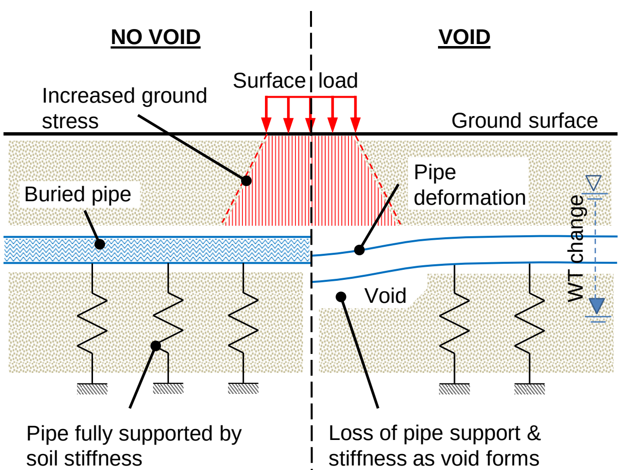

Figure 1. Soil-pipe stiffness for supported and partially supported conditions.

2 EXPERIMENTAL PROGRAMME

2.1 Centrifuge facility

The University of Sheffield small scale teaching centrifuge, herein referred to as UoS2gT/1.0, was utilised in this research. The centrifuge (Figure 2) has a nominal radius of 0.5 m and is capable of accelerating a payload of 20 kg, measuring 160 mm wide x 125 mm high x 80 mm depth, at 100 gravities (100g). The payload incorporates a viewing window which provides plane strain visualisation of the test package. The centrifuge is equipped with onboard wireless data acquisition, 2 MP camera and LED illumination for image capture, and a 2 port hydraulic rotary union for in-flight control of a 2 kN dual acting pneumatic vertical actuator. Full specification of this centrifuge is described by Black et al. (2014) and is summarised in Table 1.

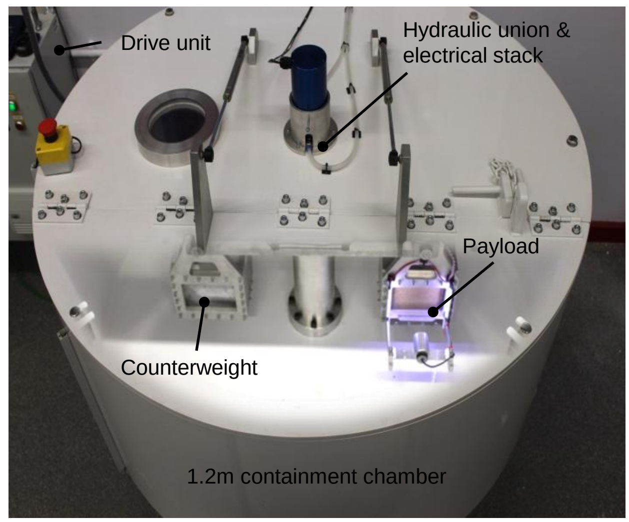

Figure 2. UoS2gT/1.0 teaching centrifuge

Table 1. UoS2-gT/1.0 centrifuge specification

Specification	Description
Radius (effective)	0.5 m (0.44 m)
Maximum payload	20 kg at 100g (2g-ton)
Maximum acceleration	100g at 20kg (≈425 RPM) 150g at 10kg (≈525 RPM)
Size of payload	W = 160 mm H = 125 mm D = 80 mm
User interfaces	2 port 10bar hydraulic union, 4 way electrical 24A slip ring
Data acquisition	8 Ch AI, 2 MP image capture, wireless communication

2.2 Model pipe

It is vital that experimental models conform to appropriate scaling relationships to provide similitude with the full scale prototype. Centrifuge scaling laws are discussed in detail by Garnier et al. (2007) and those observed in the current investigation are summarised in Table 2. Prototype stress conditions were achieved by applying an acceleration of 30g on the small scale models.

In this investigation the pipe investigated was a 0.3 m diameter (D_P) High Density Polyethylene (HDPE) flexible pipe (10 mm model scale), which is common to those frequently used in the water utilities services for new network installations or renewals. This pipe is typical of a non-trunk water main deployed in the UK. In order to capture the appropriate pipe bending response considerable effort focused on generating a model pipe that would exhibit comparable flexural stiffness as the prototype. In practice, a 0.3 m diameter HDPE has nominal wall thickness of 20 mm, Young's Modulus (E) of 0.95 GPa and flexural stiffness of 16.5 $kN.m^2$. Referring to scaling laws presented in Table 2, flexural stiffness of the model and prototype are related by $1/N^4$; hence, an appropriate model pipe geometry and material were selected to provide similitude. In this study a flexible pipe was modelled as an equivalent beam element of dimensions 10 mm high, 4 mm thick and 160 mm long. Given a Young's Modulus of 0.6 GPa, the corresponding prototype flexural stiffness was equivalent to 16.2 $kN.m^2$ which was suitable to ensure the bending characteristics of the model and prototype would be preserved. The equivalent beam geometry was selected as it was deemed advantageous in maintaining true plane strain conditions in the model tests as a cylindrical pipe element in half space may introduce out of plane torsional bending under load. At 30g the model pipe was equivalent to 0.3 m diameter and length 4.8 m at full scale.

Table 2. Centrifuge scaling laws

Parameter	Scaling law (Model/Prototype)
Gravity (m/s^2)	1*N
Length (m)	1/N
Area (m^2)	$1/N^2$
Volume (m^3)	$1/N^3$
Density (kg/m^3)	1
Stress (kN/m^2)	1
Unit Weight (kN/m^3)	1*N
Strain	1
Flexural stiffness ($kN.m^2$)	$1/N^4$

2.3 Modelling of a void

In practice voids can occur in the fill material owing to a number of possible processes such as:

(i) washing out of fines through by suffusion

(ii) moisture changes from fluctuation of the ground water table and surface infiltration causing collapse of internal soil structure

(iii) removal of supporting material due to high pressure water leaking from the mains pipe

Irrespective of the mechanism by which a void may form in practice, if they occur in the vicinity of a pipe it will result in a localised loss of support which will only serve to increase the potential for pipe deformation under applied vertical surface loading.

The formation of a 'real-time' void in a centrifuge model by any of the above processes presents a considerable technical challenge. Mair (1979) pioneered the method of deflating a fluid filled bladder/membrane to simulate sub-surface volume loss in tunnelling applications; however, owing to the small scale of the centrifuge payload this conventional void formation methodology was not viable. Several initial trial tests were conducted using ice in an attempt to provide an alternative means establishing a 'real-time propagating' void. The hypothesis of this method was to build and spin the model in elevated gravity, with an ice block buried at the desired void location; hence, an open void may be formed by self-weight arching stresses in the sand once the ice thawed. This method proved reasonable successful for small void sizes however formation of larger voids, bigger than the pipe diameter, as frequently reported in practice, were not possible.

The chosen solution to simulate a void was a compromise as it reflected the net effect of what occurs in the ground when a void is formed. Specifically, a void may be considered to be a region offering comparatively low (or zero) support to the pipe. To achieve this basic void criteria in the model tests voids were simulated using a soft sponge. This offered the ability to provide suitable support to hold back the sand material in a desired void geometry while represented a region of almost zero support to the pipe. Using this approach model spherical void geometries of 2 to 5 times the pipe diameter (D_P) were created that where 'wished-in-place' in the model during preparation (Figure 3).

2.4 Model Preparation

Prior to placing sand in the strongbox the model pipe supports were located at either ends of the viewing window and fixed into position. The strongbox was filled with Fraction B Leighton Buzzard Sand using a dry pluviation technique to ensure a uniform density. During model preparation the density of the soil sample was controlled by the dropping height, which was calibrated in previous studies to yield repeatable results at 400mm. The sand dry unit weight was 15.8 kN/m^3, particle grain size was in range of 1.18mm - 600μm. The maximum and minimum void ratios were found to be e_{max} =0.78 and e_{min} = 0.47 respectively.

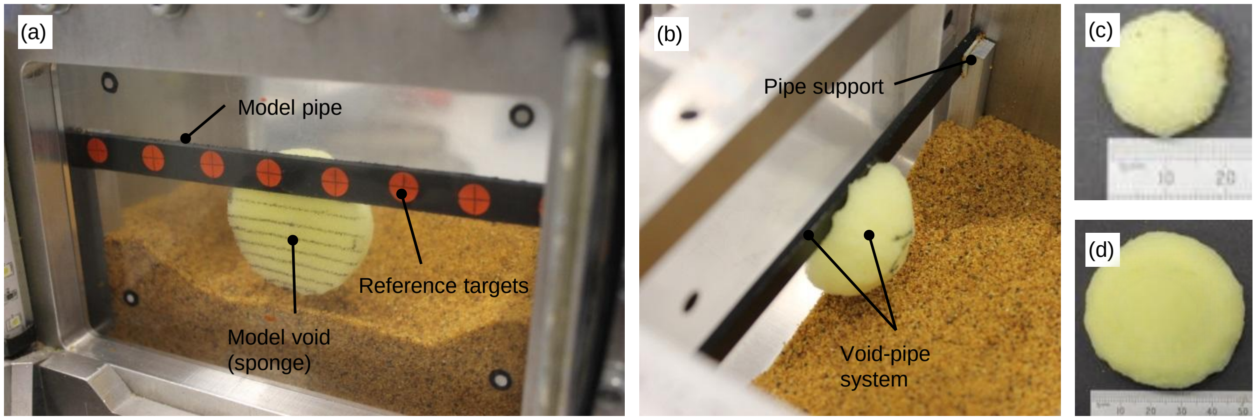

Figure 3. Modelling of a flexible pipe and void (a) pipe-void placement, (b) pipe supports, (c) $2D_P$ void and (d) $5D_P$ void.

The specific gravity of the sand solids was Gs = 2.65. A relative density, Dr, of 0.85 was repeatedly achieved during the tests.

In tests where a void and/or pipe was present, sand was filled to the required installation level at which point the void/pipe were placed with sand pluviation continuing around them. This process was carefully controlled to ensure the embedment depth and fill relative density was consistent to minimise errors associated with the 'wished-in-place' void installation method. In all tests the pipe was placed at the same burial depth with the void extending below the pipe. Reference targets were located on the model pipe to enable bending during loading to be easily identified and tracked using digital image correlation

2.5 Test programme and procedure

Five centrifuge tests were conducted which considered cases with and without a void (Table 3). The embedment depth (Z) to the pipe crown was 17 mm, 0.5 m prototype. Four void geometries of $2D_P$, $3D_P$, $4D_P$ and $5D_P$ were evaluated. In each case the void was located at the mid-span of the pipe and along the centre-line of the applied surface load. A rigid loading plate was used to simulate surface loading. The width of the footing (B) was 20 mm wide (0.6 m prototype) and was chosen to reflect a single pair of wheels on a typical truck/lorry axle moving orthogonal to the direction of the pipe. A summary of the test configuration is shown in Figure 4.

Once the model was prepared it was placed on a weighing scale to enable the mass of the counterweight to be determined. The payload was mounted into position on the beam and all electrical cables for camera and LED illumination terminated and cable tied. The vertical actuator was then mounded onto the support rails of the payload and the loading plate positioned on the soil surface. It was then locked into position using a screw clamping arrangement. During spin-up of the centrifuge an upward stress was applied to the lower actuator chamber which jacked the loading plate against the screw clamp holding it in position on top of the soil. This prevented premature loading of the soil and pipe during initial spin-up until the desired gravity level had been reached.

Once the internal safety related checks were complete the centrifuge containment lid was locked and centrifuge was accelerated to 290 RPM which was equivalent to 30 gravities at 1/3 the model height which minimised stress related errors. The image acquisition system was initiated with optimum parameters previously determined, and captured images at each load increment. Load was applied to the soil surface using by increasing the stress in the upper chamber of the vertical actuator in incremental stages of 25 kN/m^2.

Table 3. Test Info.

	Pipe	D_V (Ø)
1	Yes	None
2	Yes	$2\ D_P$
3	Yes	$3\ D_P$
4	Yes	$4\ D_P$
5	Yes	$5\ D_P$

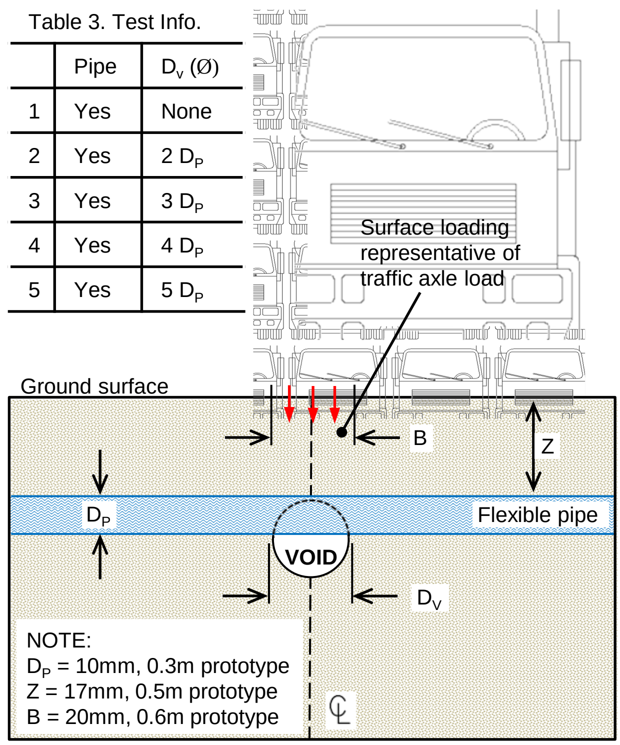

Figure 4. Test configuration and programme

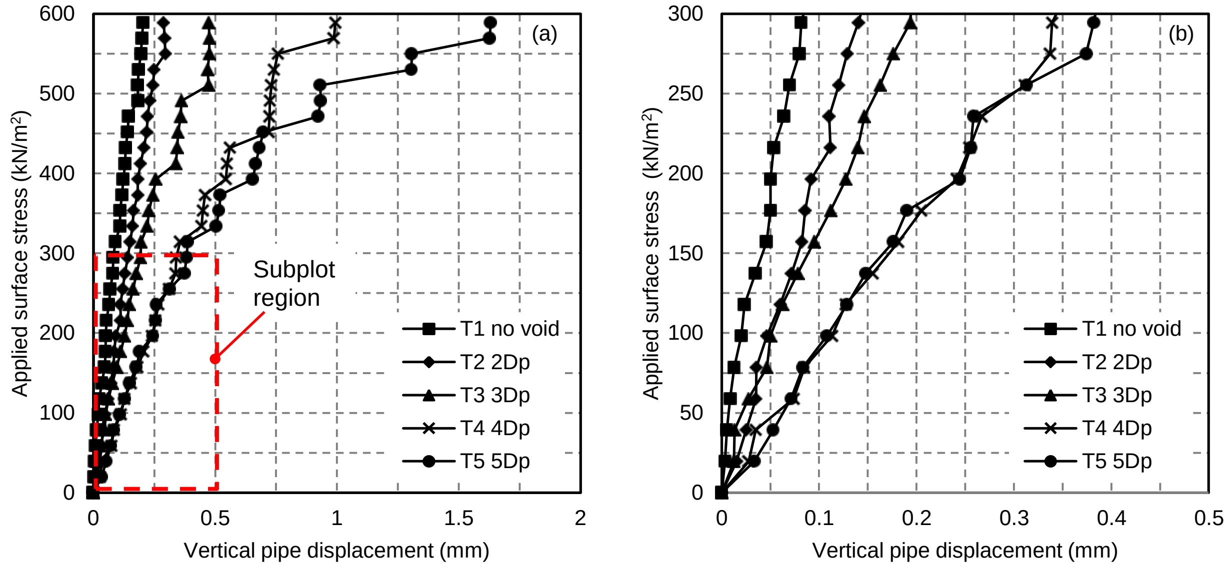

Figure 5. Vertical pipe displacement (a) full load displacement response (b) localised response.

3 RESULTS

The plane strain test configuration exposed the soil, pipe and void such that changes due to surface loading in the sub-surface regions were clearly visible in the images. Image processing was conducted using GeoPIV as developed by White et al. (2003), which is a specially adapted form of digital image correlation (DIC) for geotechnical applications. An interrogation mesh containing patches 60 pixels with spacing of 15 pixels was used globally over the images to evaluate the displacement behaviour. Various sub-data were extracted from this main dataset to evaluate specific aspects of interest such as the pipe-soil interface for examining the pipe displacement response.

3.1 Pipe deflection response

Figure 5 presents the model pipe displacements of the soil-pipe interface against the applied surface loading up to 600 kN/m^2. Comparing the data to the reference test where no void was present (Test 1), it can be observed that greater levels of pipe displacement occurred with increased void size. For example, in Test 1, 0.19 mm displacement (5.7 mm prototype at 30g) occurred at a stress of 600 kN/m^2 compared to 1.62 mm (48.6 mm prototype) when the largest void ($D_v = 5D_p$) was present beneath the pipe. Interestingly, even the smallest void ($2D_p$) yielded a considerable increase in pipe displacement approximately 50% larger than the no void condition.

Figure 5 (b) presents an enlarged subplot of the displacement response up to 300 kN/m^2 which is similar in magnitude to surface stresses that would originate from a pair of wheels on the axle of a large articulated lorry. The change in stiffness response is very evident in this enlarged plot. It is interesting to note that the initial pipe displacement response for the 2Dp and 3Dp void geometry are similar in the lower stress range up to 100 kN/m^2, this is also true in the 4Dp and 5Dp tests. This observation may indicate the existence of critical void-pipe ratios whereby at lower stresses a larger void may behave similar to that of a smaller one, as stresses may be carried by the flexible pipe thus ‘shielding’ the effects of loss of stiffness for a given void size range. Once the void exceeds this critical size further detrimental effects occur whereby greater levels of pipe displacement are generated.

3.2 Soil-pipe-void interaction mechanics

Aspects of the soil-pipe-void interaction effects are examined via the digital image correlation process that was conducted over the entire exposed surface of the model (Figure 6). Included in Figure 6 is an image for Tests 1, 2 and 4 that relate to the reference no void condition, and void geometries of $2D_p$ and $5D_p$ respectively. The image offers visual confirmation of the position and size of the void relative to the pipe, in conjunction with the corresponding vector trajectories showing the indicative soil movement in the model as determined for the applied surface loading stress of 275 kN/m^2. Note that the vector lengths are presented at a scale factor of 10 times greater to enable the soil-pipe movements to be distinguished. It is clear from the vector plot that larger levels of displacement are observed beneath the surface loading plate in T2 and T5 as the void increased. Furthermore, larger displacements of the upper soil-pipe interface are also evidence which offers additional confirmation to validate the pipe displacement responses reported in Figure 5. It is also interesting to note that the extent of vertical soil and pipe movement extends to greater horizontal distances away from the centreline of the void.

Also worth commenting on is the downward movement that can be seen within the void region in Test 5. Compression occurs immediately beneath the pipe as a consequence of the pipe deflecting under the applied surface loading. This is a clear indication that the concept of creating a region of lower stiffness than the surrounding soil using sponge to imitate a sub-surface void was suitable and highly successful.

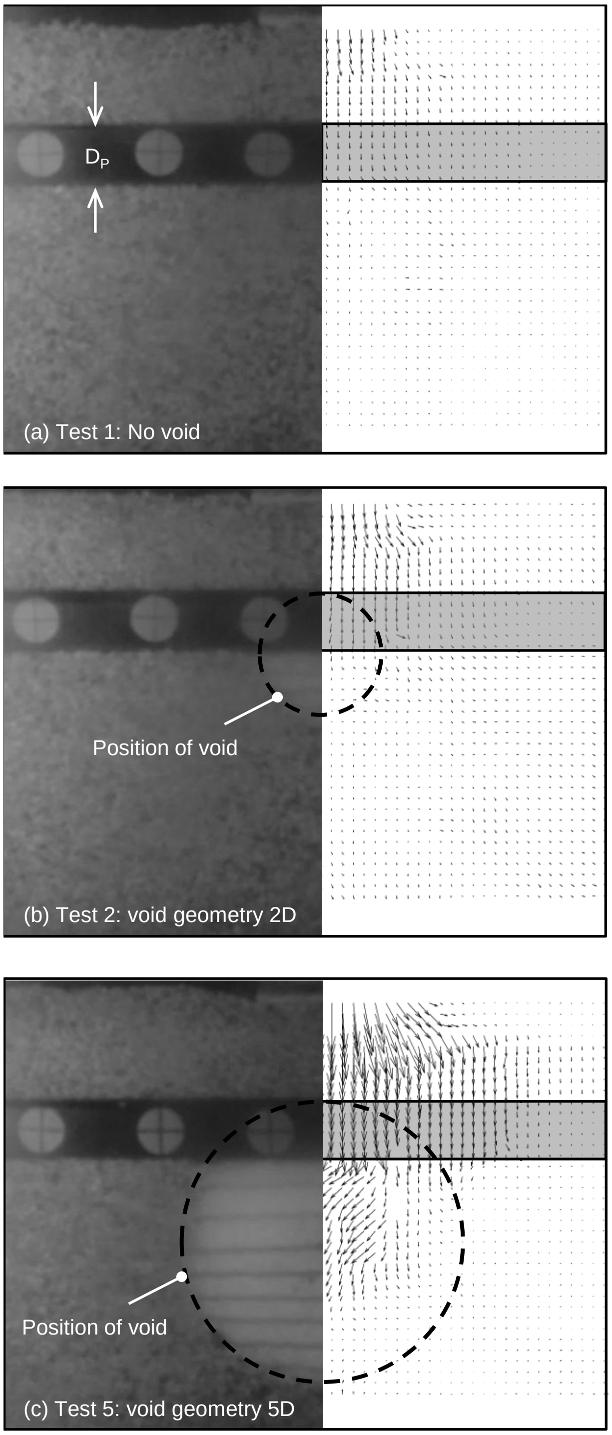

Figure 6. Soil-pipe-void interaction mechanics

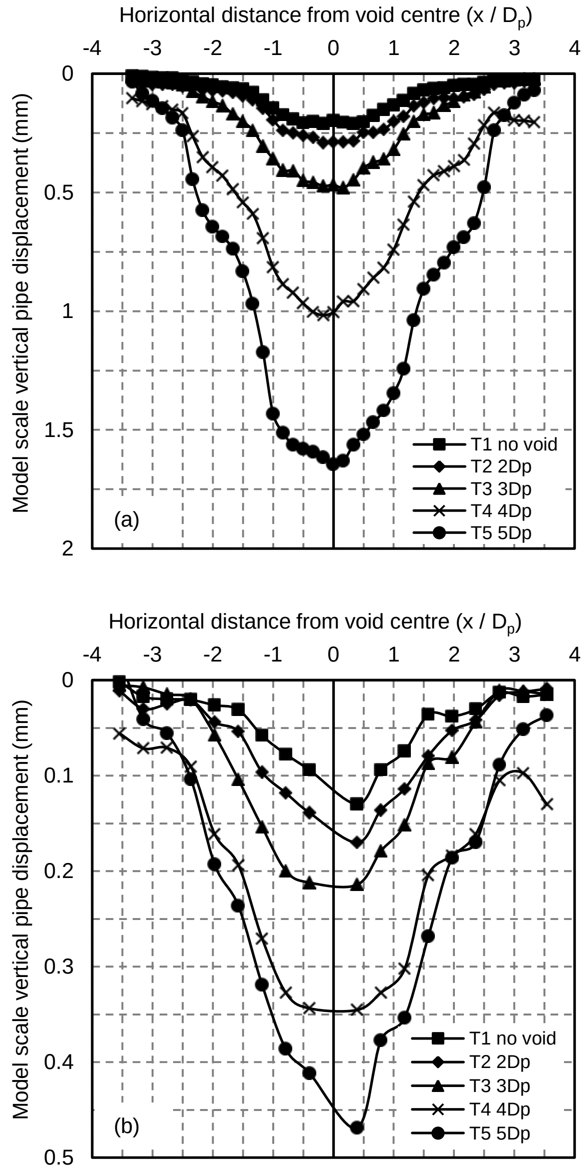

Figure 7. Pipe deflection response at (a) 600kN/m^2 and (b) 300kN/m^2 applied surface stress levels.

Figure 7 is complementary to Figure 6 whereby the magnitude of pipe interface deflection for each test at the maximum applied surface stress of 600 kN/m (Figure 7a) and more representative equivalent axle stress value of 275 kN/m^2 is presented. The trend observed at both stress ranges is clear, a larger void contributes to greater pipe displacement. Flexible pipe design criteria specifies the allowable performance limit for deflection is taken as 5% of the pipe diameter and a factor of safety of 2.5 is used on the allowable buckling pressure (AWWA 1998). Applying these criteria in the current investigation this would imply that 5% of the pipe diameter would be equivalent to a displacement of 0.5mm in the model tests.

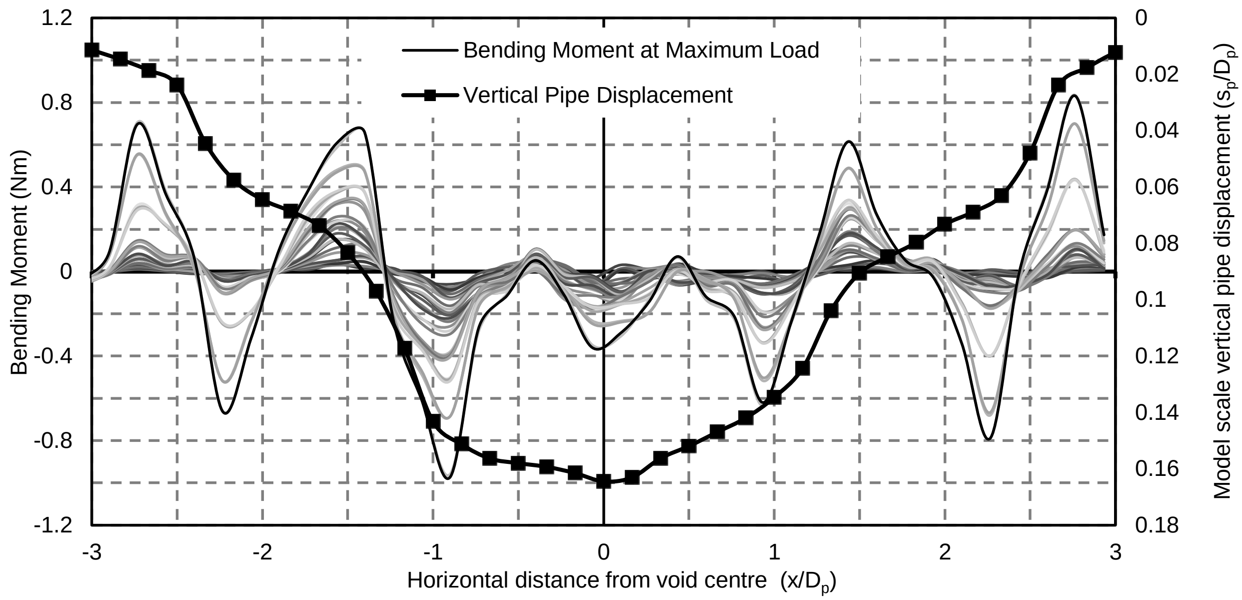

Figure 8. Pipe bending moment evolution with superimposed deflection response at the maximum load of 600 kN/m^2 in Test 5 for a void geometry of $D_v = 5\ D_p$

Reviewing Figure 7b, it is clear that at this stress level the pipe with a void in proximity of the pipe having geometry 5 D_p is on the limit of failure. Crucially however, as the magnitude of stress increases to 600 kN/m^2 Test 4 and Test 5, void size D_v = 4 and 5 D_P, have failed in deflection. Only the Tests with the smallest void sizes of 2D_p and 3D_p remain with the design criteria. Furthermore, as apparent in the soil-pipe-void interaction study presented in Figure 6 and supported by the observation in Figure 7a, tests with larger voids exhibited significantly large deflections such that they would be in jeopardy of breaching the buckling limit criteria also.

3.3 Pipe bending moment assessment

From the displacement analysis conducted using digital image correlation bending moments were determined for each pipe and void combination at the maximum applied surface stress. This was achieved by differentiating the absolute vertical pipe displacements observed at the pipe-soil interaction twice which yielded (i) the degree of downward rotation and (ii) corresponding curvature along the length of the pipe. The bending moment experienced on the pipe is expressed as

$$M = EI\kappa = EI\ \frac{d^2u}{dx^2}\ or\ EIu"(x) \qquad [1]$$

where M is the bending moment, E is the Young's Modulus of the pipe material, I is the second moment of inertia and κ is the curvature. A Taylor expansion of the displacement at x+n (equation 2) and x-n (equation 3), where x is the horizontal coordinate position of the relevant patch center in the digital image correlation matrix and n is the spacing to the subsequent patch centre, such that

$$u(x+n) = u(x) + nu'(x) + \frac{1}{2}n^2u''(x) + \frac{1}{6}n^3u'''(x) + 0(n^4) \ldots \quad [2]$$

$$u(x-n) = u(x) - nu'(x) + \frac{1}{2}n^2u''(x) - \frac{1}{6}n^3u'''(x) + 0(n^4) \ldots \quad [3]$$

Adding Equation 2 and 3 eliminates u′(x) and u‴(x) and rearranging for u″(x) gives equation 4

$$u''(x) = \frac{u(x+n) - 2u(n) + u(x-n)}{n^2} \qquad [4]$$

Bending moments are therefore determined by multiplying by *EI*. The bending moment diagram relating to Test 5 for the largest void size D_v = 5D_p is presented in Figure 8, showing both its evolution and maximum bending moment across the stress range up to 600 kN/m^2. In the figure it is evident, as expected, that the bending moment magnitude increases with applied stress. It is observed that the bending moment profile is symmetrical around the void centre which confirms the model configuration and consistent deflection behaviour observed across the unsupported section beneath the void. A number of sagging and hogging bending moments are observed that correspond to the highly variable support condition provided to the pipe by the soil and transition zone as it crossed the void area. These maximum and minimum bending moments compare favourably with the deflected profile of the pipe as shown in the superimposed plot in Figure 8.

CONCLUSIONS

A series of five centrifuge models of pipe were conducted to evaluate the effect of void size on a 0.3 m prototype flexible pipe. Four void geometries were considered ranging from 2 to 5 times the pipe diameter, simulating unsupported conditions that were benchmarked to the reference case of no void. The results of the investigation indicate that the magnitude of pipe deflection increased significantly in the presence of a void and that the magnitude of deflection increased with void size. Also presented was the soil displacement behaviour from image analysis whereby it was observed that the level of soil displacement from a surface loading plate increased with void size which served to increase the extent of loading on the pipe. Also confirmed was the suitable methodology implemented of using a sponge to simulate a sub-surface region of reduced stiffness mimicking a prototype void. Bending moments were evaluated in the pipe and were found to be both sagging and hogging which corresponded to the points of inflection from the pipe deflection response. The relevant deflection of the pipe was found to exceed the allowable deflection criteria for void sizes larger than 3 times the pipe diameter. This study has served to provide valuable preliminary insight of the behaviour of flexible utility pipes in the presence of a void subjected to surface loading. Additional tests are ongoing in this area and it is hoped that greater understanding will be generated to develop appropriate design and management plans of the future to boost the resilience of this critical infrastructure asset.

ACKNOWLEDGEMENTS

The experiments reported in this paper were completed using the UoS2gT/1.0 teaching centrifuge that was developed through funding by the National Higher Education STEM Programme. Continued support by Thomas Broadbent and Son Ltd. to the Centre for Energy & Infrastructure operation and large 4m diameter centrifuge facility are gratefully acknowledged. The contribution by the Department of Civil & Structural Engineering technical staff, Paul Osborne, Mark Foster, Alex Cargill, Dave Callaghan and Dr. Paul Bentley (Electronics) for in-house technical support is also acknowledged.

REFERENCES

American Society of Testing and Materials (ASTM) C 443-05. 2005. Standard Specification for Joints for Circular Concrete Pipe and Manholes, Using Rubber Gasket, *ASTM International*, 100 Barr Harbor Drive, PO BoxC700, West Conshohocken, PA, 19428-2959 USA

American Water Works Association (AWWA). 1998. Fiberglass pipe design. 1st ed. *American Water Works Association*, Denver, Colo. Standards Manual M45.

Becerril García, D., and Moore, I.D. 2015. Behaviour of bell and spigot joints in reinforced concrete pipes. Canadian Geotechnical Journal, 52.

Black, J.A. Baker, N. and Ainsworth, A. 2014. Development of a small scale teaching centrifuge. *Physical Modelling in Geotechnics - Proceedings of the 8th International Conference on Physical Modelling in Geotechnics* 2014, ICPMG 2014.

Brachman, R.W.I., McLeod, H.A., Moore, I.D., and Take, W.A. 2010. Three dimensional ground displacements from static pipe bursting in stiff clay. *Canadian Geotechnical Journal*, 47(4): 439–450. doi:10.1139/T09-118.

British Standards Institution (BSI). 1998. BS EN 1295-1:1997 Structural design of buried pipelines under various conditions of loading: General requirements.

Garnier, J. Gaudin, C. Springman, S.M. Culligan, P.J. Goodings, D.J. Konig, D. Kutter, B.L, Phillips, R. Randolph, M.F. Thorel, L. 2007. Catalogue of scaling laws and similitude questions in geotechnical centrifuge modelling 7 (3), *International Journal of Physical Modelling in Geotechnics*, pp. 1–23, ISSN: 1346-213X, E-ISSN: 2042-6550.

Kellogg, C. G. 1993. Vertical Earth Loads on Buried Engineered Works. *Journal of Geotechnical Engineering*, Vol. 119, No. 3. 487-506.

Klar, A., Vorster, T. E., Soga, K., and Mair, R. J. 2005. Soil-pipe Interaction due to Tunnelling: Comparison between Winkler and Elastic Contimuum Solutions. *Geotechnique*, Vol. 55. 461-466.

Mair, R. J. 1979. Centrifugal modelling of tunnel construction in soft clay. PhD thesis, *University of Cambridge*.

Marshall, A. M., 2009. Tunnelling in Sand and its Effect on Pipelines and Piles. *Univeristy of Cambridge*.

Rajani, B., and Tesfamariam, S. 2004. Uncoupled Axial, Flexural, and Circumferential Pipe-soil Interaction Analyses of Partially Supported Jointed Water Mains. *Canadian Journal of Geotechnics*, vol. 41. 997-1010.

Rakitin, B. and Xu, M. 2014. Centrifuge modeling of large-diameter underground pipes subjected to heavy traffic loads. *Canadian Geotechnical Journal*. 51: 353–368.

Ratnayaka, D. D. 2009. Twort's Water Supply. Oxford.

Tan, Z., & Moore, I. D. 2007. Effect of Backfill Erosion on Moments in Buried Rigid Pipes. *Transportation Research Board Annual Conference*. Washington DC.

Zhang, C., Yu, J., & Huang, M. 2012. Effects of Tunnelling on Existing Pipelines in Layered Soils. Computers and *Geotechnics*, vol. 43. 12-25.

White, D., Take, W., and Bolton, M., 2003, Soil Deformation Measurement Using Particle Image Velocimetry (PIV) and Photogrammetry, *Geotechnique*, Vol. 53, No. 7. 619–631.